Design of illumination and projection optics for projectors with single digital micromirror devices

Chong-Min Chang and Han-Ping D. Shieh

We present a new optical system design for a projector with a single digital micromirror device (Texas Instruments Digital Micromirror Device) that improves on previous designs in terms of optical efficiency, uniformity, and contrast while yielding a low-profile and compact system. A rod integrator is incorporated with a compact relay system to maximize light efficiency and to increase illumination uniformity. The uniformity achieved by the optimized optical system was calculated to be 94%. In addition, this unique light-separator design has dual output channels to increase the image contrast by steering the off-state light away from the projection lens. This projector design provides very efficient light utilization, and we discuss how the geometrical optical efficiency of the system can be boosted to approach the theoretical maximum. © 2000 Optical Society of America

OCIS codes: 080.2740, 080.3620, 220.2740, 220.3620, 120.2040, 230.6120.

1. Introduction

Projectors offer a good solution for large screen displays by producing high-quality images with a compact and lightweight apparatus.[1–7] In recent years projection displays based on the Texas Instruments Digital Micromirror Device (DMD) have achieved much success, since they avoid the bulky polarization optics required by liquid-crystal display (LCD) projectors. At the same time, the high fill factor and pixel density of the DMD can yield projector systems with excellent characteristics in terms of light utilization, resolution, and image quality. There are still issues and improvements stemming from the small size of the light valve and its unique method of operation that are yet to be addressed for high-performance projector systems.

One issue arises from the unique reflective operation of the DMD. Because of the narrow tilt angle of the micromirrors, a special optical design is required for adequate separation of the incident and the reflected light beams. For light path interference to be eliminated, an offset solution has been adopted in some designs to separate the light bundles for the

single-DMD projectors.[1–3] In this relatively intricate arrangement, a projection lens with an unusually small entrance pupil near the DMD is needed to leave adequate space for the illumination optics. Moreover, the illumination system incorporated with the projection lens must use a truncated condenser lens. The projection lens diameter, especially at the screen side, increases in proportion to the DMD size. Consequently, the overall system size increases substantially to accommodate a huge projection lens when the DMD size grows with its resolution.

Another issue is associated with the common problems of low efficiency and poor uniformity in projection systems. To provide an adequate contrast ratio, the F/number of the projection lenses for DMD-based projectors has to be no smaller than $F/3$, corresponding to the DMD title angle of $\pm 10°$.[1–3] Because of the restriction on the F/number, the small size of the DMD makes efficient light coupling from the light source more difficult. The optical system conventionally used in single-DMD projectors is the Abbe configuration, which offers the advantages of portability and low cost.[1–3] Unfortunately, this configuration images the nonuniform arc source directly onto the DMD, resulting in a higher light intensity at the center of the illumination beam than at its outer edges. A circular light profile illuminating a rectangular light valve is also not an efficient use of the light. A lens-array integrator has been proposed to improve both light efficiency and uniformity.[8–9] However, the scheme requires two intricate lens-array plates, each typically containing between 10

C.-M. Chang (u8424505@cc.nctu.edu.tw) and H.-P. D. Shieh are with the Institute of Electro-Optical Engineering, National Chiao Tung University, Hsinchu, Taiwan 30050.
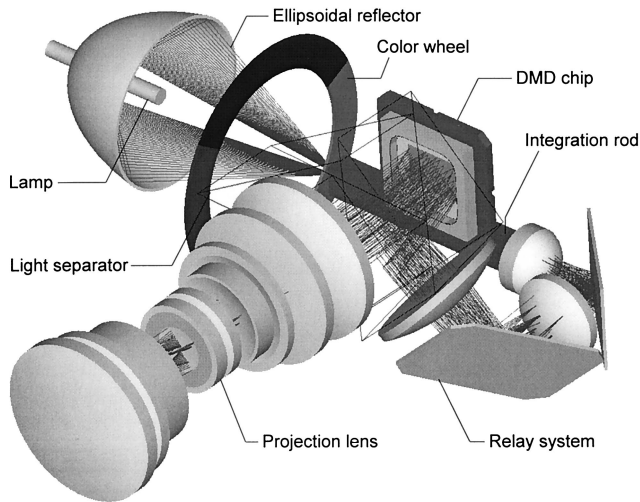
Fig. 1. Optical layout of the projection system with a single DMD chip.

Fig. 2. Illumination system layout.

and 1000 lenses arrayed in two dimensions, to accomplish the functions. Furthermore, an additional condenser lens, positioned between the color wheel and the integrator, is needed to collimate the colored beam.

In this paper we describe a new optical system design that offers solutions to the problems mentioned above. The new design employs a unique light separator to maximize the contrast ratio and a compact illumination system incorporated with a relay system to deliver higher brightness and uniformity. The paper is organized in two main sections followed by concluding remarks. The system design for the projector is given in Section 2, and the design evaluation results are given in Section 3.

2. Optical System

The optical system layout for our single-DMD projector is shown in Fig. 1. The system consists of three main subsystems: an illumination system, a relay system, and a projection system. The light from the lamp is collected by the illumination system and passes through the relay system toward the DMD chip. The micromirrors arrayed on the chip are controlled by electrostatic force to steer the reflected light from each pixel either into or away from the entrance pupil of the projection lens.[1–3] Each of the subsystems are treated in turn in the discussion below.

A. Illumination System

The illumination system, shown in Fig. 2, comprises a short-arc lamp, an ellipsoidal reflector, a color wheel, and a pillarlike integration rod. The ellipsoidal reflector converges the light emitted from the arc source located at the first focus of the reflector onto the color wheel. After passing through the color wheel, the colored beam is incident on the entrance facet of the integration rod.

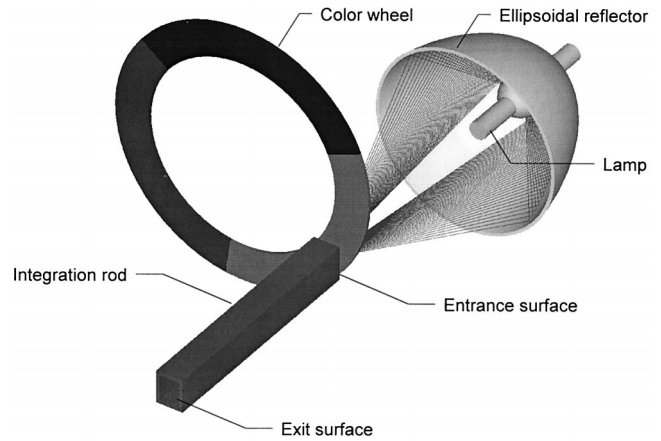The integration rod is an optical device shaped like a rectangular pillar.[10–12] It can be either a glass rod or a hollow, mirrored tube with a rectangular cross section matching the aspect ratio of the light valve. By way of multiple reflections from the internal surfaces, the circular light profile is transformed into a rectangular one. In addition, the rod functions as a scrambler to modify the luminous distribution of the light beam. The nonuniform arc source is imaged through the color wheel onto the entrance surface of the rod. The resulting illumination at the exit surface is an overlap of the checkerboard array of the source images caused by multiple reflections within the rod. The convergence angle of the beam from the reflector and the length of the rod determine the number of the reflected images. The overlap of these virtual sources effectively smoothes out the nonuniform intensity profile of the arc lamp source, producing a uniform flattop beam profile on the exit side of the rod. The more virtual sources created by reflections in the rod, the higher the degree of uniformity.

B. Relay System

After leaving the integration rod, the light is directed by the relay system toward the DMD. As shown in Fig. 1, the relay system is composed of the first lens group on the exit side of the rod, the second lens group near the light valve, and the two folding mirrors.[10–12] The relay system employs the so-called Köehler configuration in conjunction with a telecentric design to produce uniform illumination on the DMD surface. In this configuration the exit surface of the rod is imaged onto the surface of the DMD. At the same time, the multiple virtual sources at the entrance plane of the rod are imaged onto the entrance pupil of the projection lens. The design is telecentric because the virtual images of the source formed by the first lens group fall exactly at the focal plane of the secondary lens group. With this arrangement, the light illuminating the DMD is essentially collimated, and the light bundles are incident on each micromirror at the same angle. The configuration gives a uniform distribution on the light valve

with an optimum rectangular cross section matched to the aspect ratio of the DMD and provides the adequate light bundles for the telecentric projection lens. Quantitative values for the efficiency and uniformity are calculated in Section 3. In contrast, the Abbe configuration conventionally used in single-DMD projectors images the arc source onto the DMD plane directly such that the irregularities in the arc are evident in the displayed image.[2,3]

C. Projection System

To eliminate the light path interference and to maximize the contrast ratio, we incorporated a new light separator into the projection system. The light separator is an integral feature of the compound prism system to steer the light onto and away from the DMD. As shown in Fig. 3, the prism system comprises three transparent prisms, between which there are two air gaps. Total internal reflection (TIR) at the interface between the prism and the air gap is utilized to separate the light bundles by angle. The advantage of the light separation by TIR is that the s- or the p-polarization split effect can be avoided,[5] because the reflectance at the TIR surface is 100% for the s- and the p-polarization states over the wavelengths. However, the transmission at the angle smaller than but close to the critical angle, θ_C, must be enhanced by high-efficient antireflection coatings, which is a challenge in the coating design.

The main idea of the light separator design is to utilize two TIR surfaces to separate three light beams. As shown in Figs. 3(a) and 3(b), the first TIR surface, near the DMD, is used to separate the incident and the reflected beams, and the second TIR surface, near the projection lens, creates dual output channels for the on-state and the off-state reflected beams. In the prism system the orientation angles of these TIR surfaces are determined by the title angle of the DMD and the refractive index of the prism. The first TIR surface is orientated such that the illumination beam strikes this surface at an angle larger than θ_C, but the on- and the off-state beams are incident on this surface at an angle smaller than θ_C. Thus the illumination beam and the two reflection beams are separated. The second TIR surface is tilted such that the on-state beam encounters this surface at an angle smaller than θ_C, but the off-state beam is incident on this surface at an angle larger than θ_C. Therefore, the on-state reflection beam passes through the air gap, and the off-state light is directed away from the projection lens at roughly 90°. Since the light power of the illumination is extremely high, the off-state beam passing through the top portion of the prism assembly has to be absorbed to prevent irregular reflection or scattering inside the optical system housing. As a result, the amount of stray light entering the projection beam is substantially reduced, and the contrast ratio in the projection beam is increased.

In actuality, the on-state beam and the off-state beam are not the only beams reflected from the DMD. Additionally, the light incident on the fixed struc-
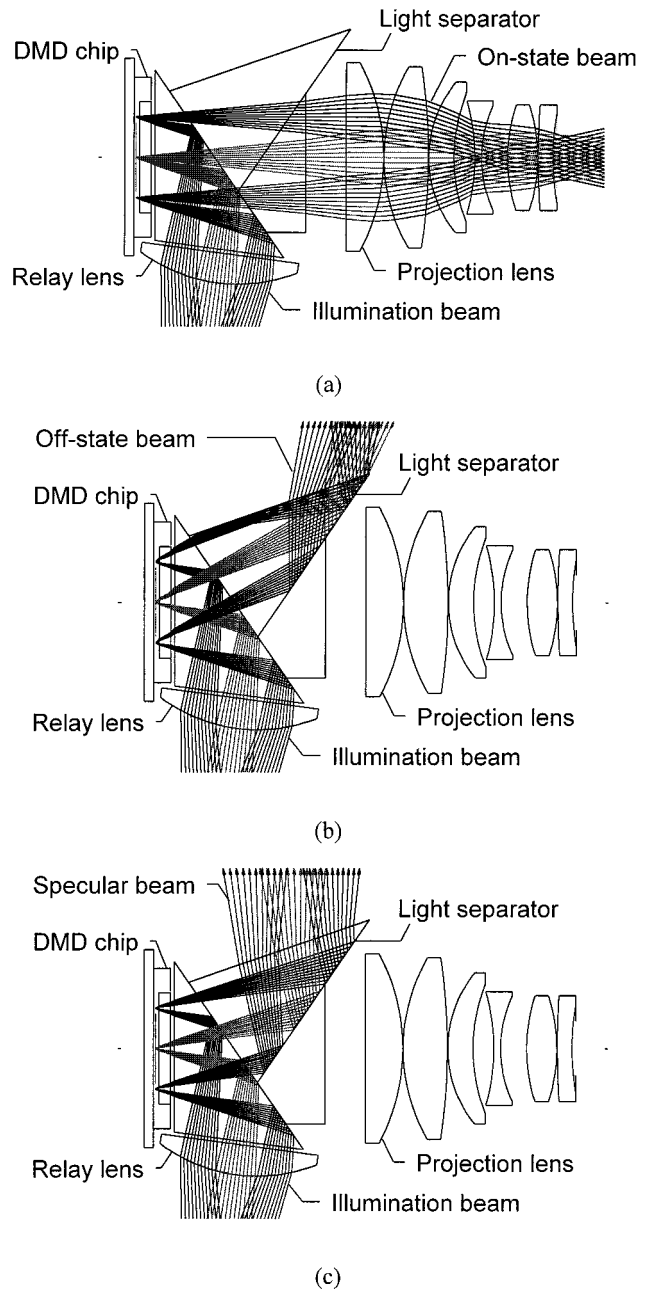

(a)

(b)

(c)

Fig. 3. Arrangement of the DMD chip, the light separator, and the projection lens. (a) On-state beam is directed into the entrance pupil of the projection lens. (b) Off-state beam and (c) specular beam are steered away from projection lens at roughly 90°.

tures of the DMD surface, e.g., the hinge posts and the silicon substrate, is specularly reflected in neither the on nor off state. In the first-order analysis, the specular beam can be treated as the light reflected from the plane parallel to the DMD surface. As shown in Fig. 3(c), the design of the light separator also directs this unwanted light away from the projection lens to further enhance the contrast ratio.

Another advantage of using the light-separator design is that the optical system can be made telecentric. As illustrated in Fig. 3, the illumination beams
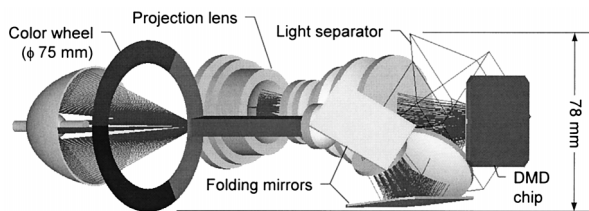
Fig. 4. Schematic diagram of an alternative optical layout as implemented within a low-profile package.

have the same angles of incidence on each micromirror, and the projection lens is telecentric on the DMD side. The exit pupil of the projection lens is positioned at infinity, and the corresponding chief rays on the DMD side are parallel to the optical axis. This approach cannot be practically accommodated in the offset design because the telecentric projection lens adjacent to the DMD has a comparatively larger diameter, resulting in the interference with the illumination optics.[2,3]

Additionally, the optical configuration permits an ultraportable design. The two folding mirrors incorporated in the relay system provide an alternatively compact optical layout. Figure 4 shows the arrangement of the lenses and the folding mirrors as implemented within a low-profile package. The axis of the illumination system is parallel and close to that of the projection assembly, resulting in a low, 78-mm profile and a footprint of 220 mm × 175 mm.

3. System Evaluation

The performance of this projection system has been evaluated in terms of its geometrical optical efficiency and uniformity delivered to the screen.[13–17] The heart of the optical system is the DMD chip with its 1024 × 768 pixel resolution, the 0.9-in. diagonal aperture, and the 4:3 aspect ratio. The optical specifications of the system are given in Table 1.

A. Geometrical Optical Efficiency

The total luminous flux delivered to the screen is a primary concern for the optical system. Numerous key parameters among the optical components must be carefully determined to achieve the design goal. For a single-DMD projection system, the light efficiency is determined by the optical efficiency of the DMD, η_{DMD}, the spectral efficiency of the optical elements, η_{SPEC}, and the overall geometrical optical

Table 2. Optical Efficiency of the DMD

Item	Parameter	Value (%)
DMD	Fill factor	89.0
	Switching time	92.0
	Reflectivity	88.0
	Diffraction efficiency	85.0
Optical efficiency	η_{DMD}	61.2

efficiency, η_{GEO}.[1,4] The total light throughput of the system, F_{SYS}, is the product of these efficiencies, and the output flux of the lamp, F_{LAMP}, is given by

$$F_{SYS} = (\eta_{DMD} \times \eta_{SPEC} \times \eta_{GEO}) \times F_{LAMP}. \tag{1}$$

The efficiency of the DMD, η_{DMD}, determined by the fill factor, switching time, reflectivity, and diffraction factors, is 61%, as given in Table 2.[1] The spectral efficiencies of optical components, based on the measurement of commercial optics used in an early-projection system, are estimated in Table 3. The projection system uses the color sequential operation with the temporal duty cycle of 33% for each color, so the effective spectral efficiency of a color wheel is only 28.5%.[4] Taking together these losses associated with transmission, reflection, and absorption of the optical components and the temporal modulation by the color wheel, the overall spectral efficiency, η_{SPEC}, is estimated to be 16%.

With DMD and spectral contributions ignored, the overall geometrical optical efficiency, η_{GEO} is the ratio of the light flux delivered by the entire projection system to the total flux emitted from the lamp.[13–16] The evaluation of η_{GEO} was performed by the Advanced Systems Analysis Program (ASAP) ray-tracing program.[17] Based on the optimized optical system, full three-dimensional geometrical models of the optical and the mechanical components were created for ray-tracing analysis. Instead of an ideal point source an extended source model was used as the light source, where the number of rays per unit length along the axis was uniformly distributed within a cylinder of finite length, Z_{ARC}, and diameter, D_{ARC}. Figure 5 is a schematic diagram showing the ellipsoidal reflector and the arc cylinder. Because the discharge plasma of the arc source can be treated as a superposition of the uniform cylindrical emitters with appropriate spatial apodization, this two-parameter light source model is useful for character-

Table 1. Optical Specifications

Item	Parameter	Value
DMD chip	Aspect ratio	4:3
	Resolution	1024 × 768
	Pixel size (μm^2)	17 × 17
	Diagonal (in.)	0.9
Projection lens	Focal length (mm)	37
	F/number	F/3
Screen	Distance (m)	2.4
	Diagonal (in.)	57

Table 3. Spectral Efficiency of the Opitcal Elements

Item	Parameter	Value (%)
Illumination system	Ellipsoid reflector	90.0
	Rod integrator	90.0
Relay system	Relay lenses	94.0
	Folding mirrors	96.0
Projection system	Projection lens	90.0
	Light separator	88.0
Color wheel	Color filters	28.5
Spectral efficiency	η_{SPEC}	16.5
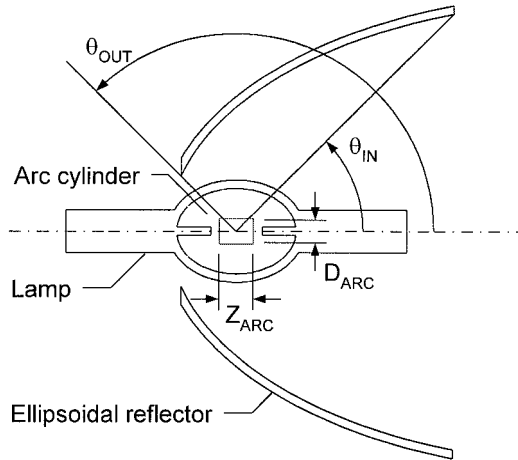
Fig. 5. Schematic diagram showing the ellipsoidal reflector and the arc cylinder.

Fig. 6. Collection and coupling efficiencies $\eta_{\text{COLLECTION}}$ and η_{COUPLING} versus Z_{ARC} and D_{ARC}.

izing arc lamps for the evaluation of η_{GEO}.[13–17] Furthermore, the radiant intensity distribution of the source, I_{ARC}, that defines the far-field properties is given by

$$I_{\text{ARC}}(\theta, \phi) = I_o \sin \theta, \qquad (2)$$

where θ is the angle from the cylinder axis, ϕ is the angle around the axis, and I_o is the peak intensity. Since the light emitted from the arc source is widely divergent, the maximum light flux collected by a reflector imposes a theoretical limitation on η_{GEO}. With a reflector with an inner collection angle θ_{IN} and an outer angle θ_{OUT}, the maximum light flux delivered by a projection system, F_{MAX}, can be evaluated by the integration of Eq. (2) over the solid angle of the reflector and is given by

$$F_{\text{MAX}} = \iint I_{\text{ARC}}(\theta, \phi) d\Omega$$
$$= \pi I_o \left[\theta_{\text{OUT}} - \theta_{\text{IN}} - \frac{\sin(2\theta_{\text{OUT}}) - \sin(2\theta_{\text{IN}})}{2} \right]. \qquad (3)$$

For a typical deep aspheric reflector with $\theta_{\text{IN}} = 45°$ and $\theta_{\text{OUT}} = 135°$ the theoretical maximum η_{GEO} that can be achieved is approximately 82%; i.e., $\eta_{\text{GEO}} \leq F_{\text{MAX}}/F_{\text{LAMP}} = 82°$.

For convenience in the analysis, the overall optical geometrical efficiency, η_{GEO}, was divided into the collection efficiency, $\eta_{\text{COLLECTION}}$, and the coupling efficiency, η_{COUPLING}. The collection efficiency, $\eta_{\text{COLLECTION}}$, determined mainly by the light source and the reflector, is the ratio of the usable light flux entering the integration rod to the total flux emitted from the lamp. On the other hand, the coupling efficiency, η_{COUPLING}, is the percentage of the usable light flux that can be coupled into the projection system and is related to the relay system, the light separator, and the projection lens. The efficiencies, $\eta_{\text{COLLECTION}}$ and η_{COUPLING}, as functions of Z_{ARC} and D_{ARC}, are plotted in Fig. 6. It can be seen that the

usable light flux entering the integration rod increases as Z_{ARC} decreases. The collection efficiencies, $\eta_{\text{COLLECTION}}$, independent of the value of D_{ARC}, degenerate into the efficiency of an ideal point source as Z_{ARC} decreases to less than 0.6 mm. For high efficiency to be achieved, the relay system must be well corrected and have an étendue close to that of the DMD, thus preventing the light flux loss. Figure 6 also shows that the values of η_{COUPLING} are approximately 96% and are almost independent of the arc parameters, establishing that the usable light can be efficiently coupled into the projection by the relay system.

The overall geometrical optical efficiency, η_{GEO}, plotted in Fig. 7 as a function of Z_{ARC} for various values of D_{ARC}, is the combined effect of the collection and the coupling efficiencies. The curves of η_{GEO} are parallel and close to those of $\eta_{\text{COLLECTION}}$. The curves also show that the overall efficiency, η_{GEO}, is determined primarily by the amount of light collected into the integrating rod by the reflector and that the optical system itself provides very efficient light uti-
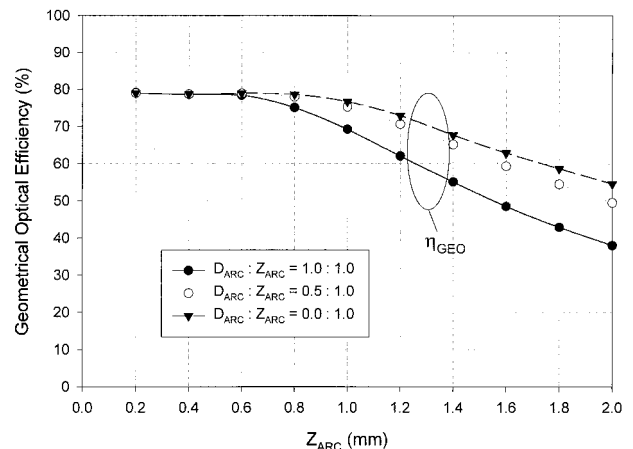

Fig. 7. Geometrical optical efficiency η_{GEO} versus Z_{ARC} and D_{ARC}.
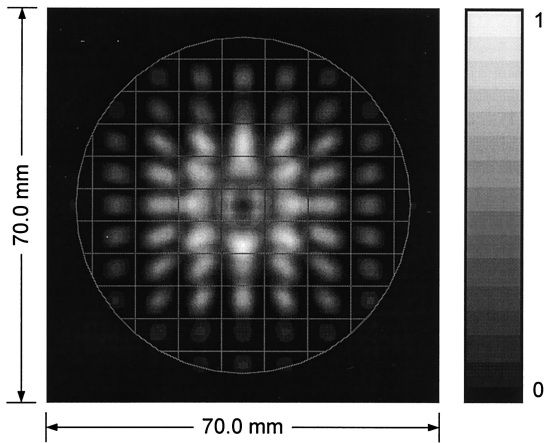
Fig. 8. Calculated image of the virtual sources arrayed at the entrance surface of the rod. A circular grid overlaid on the source array represents the collection angle of the projection lens.

lization. When $Z_{ARC} = 1.0$ mm, $\eta_{GEO} > 68\%$ can be achieved. For $Z_{ARC} < 0.6$ mm, η_{GEO} can be boosted to 78%, very nearly approaching the theoretical maximum of 82%.

B. Irradiance Uniformity

The irradiance uniformity of the system was evaluated with an arc source model of a commercially available metal halide lamp, whose gap between the electrodes is 1.2 mm.[18] The emitting discharge plasma between the electrodes was modeled as a superposition of a series of uniform cylindrical emitters. For the best source fidelity to be obtained, these emitting volumes were apodized according to the measured spatial and angular distributions of the lamp. With the ASAP ray-tracing program,[17] 1,000,000 rays were created at the source model, and then traced nonsequentially through the geometrical model of the optical system.

Figure 8 shows the calculated image of the virtual sources arrayed at the entrance surface of the integration rod, which is also the distribution imaged onto the entrance pupil of the projection lens. The gray level in the diagram is proportional to the calculated irradiance. The multiple virtual sources are created by the reflections within the integration rod. A circular grid overlaid on the source array represents the collection angle of the $F/3$ projection lens referred back to the entrance face of the rod. The circular beam profile was divided into many rectangles that were equal to the cross section of the rod. It can be seen that all of the light sources fall within the usable aperture. Although each individual source is not uniform at the entrance plane of the rod, the combined contribution of these sources effectively smoothes out the variations and gives a very uniform irradiance distribution at the exit surface.

This exit distribution from the rod is imaged onto the DMD surface by the relay system and is again imaged onto the screen by the projection lens. Because the exit surface of the rod, the DMD surface,
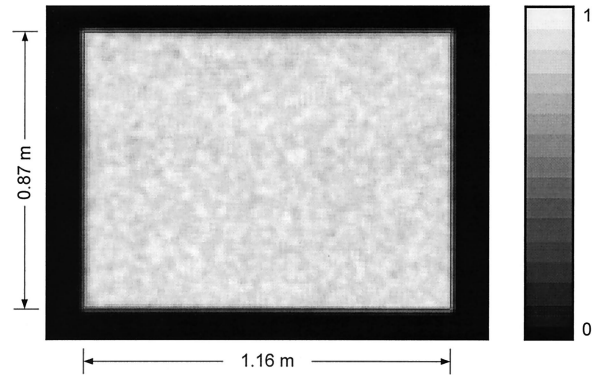

Fig. 9. Calculated irradiance distribution on the screen (1.16 m × 0.87 m).

and the screen are mutually conjugate planes, the spatial distributions of the light at these surfaces are the same. Figure 9 shows the calculated irradiance distribution on the screen. The cross-sectional profiles of the screen irradiance along the horizontal and the vertical directions are shown in Fig. 10. It can
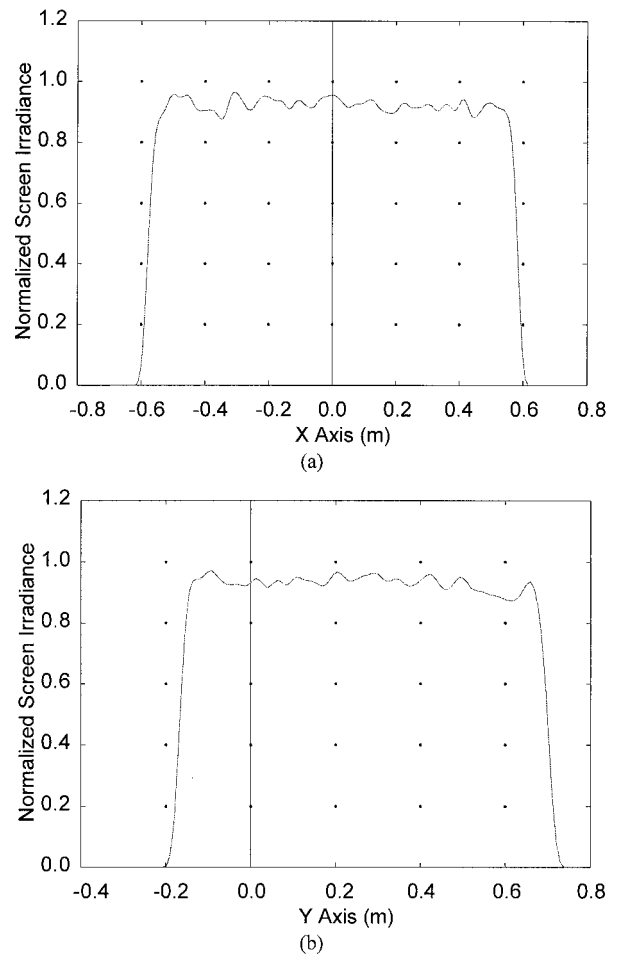

Fig. 10. (a) Horizontal and (b) vertical profiles of the normalized screen irradiance. Note that the projection axis is titled upward above the horizontal to raise the projected image, and thus the vertical profile is not symmetrical.

be seen that the screen irradiance has sharp edges and a relatively flat distribution. The irradiance variation is approximately 94% by the ANSI nine-point test method, where the irradiance at each of the nine points is calculated and then normalized to that of the maximum value.[19]

4. Conclusions

A new system design for single-DMD projectors was proposed to improve efficiency, uniformity, contrast, and compactness. An integration rod is used in the illumination system to achieve a uniform illumination free of hot spots and matched to the cross section of the DMD. The relay system employs the Köehler configuration with a telecentric design that images the exit surface of the integration rod onto the light valve to provide uniform illumination and the same incidence angles for rays at all locations on the DMD surface. The projection optics incorporates a unique light separator to eliminate the light path interference between the entering and the exiting beams. The light separator can further improve contrast by steering the off-state beam and the specular beam out of the projection path at 90° to minimize stray light entering the projection lens. In addition, a compact optical layout is suggested to produce a low-profile optical system. The final system has a height of 78 mm and a footprint of 220 mm × 175 mm.

An optical coupling efficiency of 96% and a uniformity of 94% are achieved with the design. The overall geometrical optical efficiency of the entire system with a short arc lamp can be boosted to the value of 78%, approaching the theoretical maximum of 82%. These features and results represent a substantial improvement over conventional single-chip projection system designs.

References

1. L. J. Hornbeck, "Digital light processing for high-brightness, high-resolution applications," in *Projection Display III*, M. H. Wu, ed., Proc. SPIE **3013**, 27–40 (1997).
2. G. H. Moss, R. G. Fielding, M. Kavanagh, and B. R. Critchley, "A high-luminance large-screen projection system using the digital micromirror device (DMD)," in *SID '96 International Symposium Digest of Technical Papers* (Society for Information Display, Santa Ana, Calif., 1996), pp. 907–910.
3. H. C. Burstyn, D. Meyerhofer, and P. M. Heyman, "The design of high-efficiency high-resolution projectors with the digital micromirror device," in *SID '94 International Symposium Digest of Technical Papers* (Society for Information Display, Santa Ana, Calif., 1994), pp. 677–680.
4. G. S. Pettitt, A. DeLong, and A. Harriman, "Colorimetric performance analysis for a sequential color DLP projector system," in *SID '96 International Symposium Digest of Technical Papers* (Society for Information Display, Santa Ana, Calif., 1996), 510–513.
5. P. M. Alt, "Single crystal silicon for high resolution displays," in *Proceedings of the Seventeenth International Display Research Conference* (Society for Information Display, Santa Ana, Calif.,1997), pp. 19–24.
6. S. Shikama, H. Kida, A. Daijogo, Y. Maemura, and M. Kondo, "A compact LCD rear projector using a new bent-lens optical system," in *SID '93 International Symposium Digest of Technical Papers* (Society for Information Display, Playa del Rey, Calif., 1993), pp. 295–298.
7. Y. Itoh, J. I. Nakamura, K. Yoneno, H. Kamakura, and N. Okamoto, "Ultra-high-efficiency LC projector using a polarized light illumination system," in *SID '97 International Symposium Digest of Technical Papers* (Society for Information Display, Santa Ana, Calif., 1997), pp. 993–996.
8. H. J. van den Brandt and A. G. Timmers, "Optical illumination system and projection apparatus comprising such a system," U. S. patent 5,098,184 (24 March 1992).
9. P. J. Janssen and J. A. Shimizu, "High contrast illumination system for video projection," U.S. patent 5,442,414 (15 August 1995).
10. C. M. Chang, K. W. Lin, K. V. Chen, S. M. Chen, and H. P. Shieh, "A uniform rectangular illumination optical system for liquid crystal light valve projectors," in *Proceedings of the Sixteenth International Display Research Conference* (Society for Information Display, Santa Ana, Calif.,1996), pp. 257–260.
11. K. W. Lin, K. V. Chen, S. M. Chen, H. P. Shieh, and C. M. Chang, "High optical throughput liquid-crystal projection display system," U.S. patent 5, 748,376 (5 May 1998).
12. Y. Kudo and K. Matsumoto, "Illumination optical device," U.S. patent 4,918,583 (17 April 1990).
13. C. Nicolas, B. Loiseaux, and J. P. Huignard, "Analysis of the optical components in liquid crystal projectors by their geometrical extend," in *Proceedings of the Thirteenth International Display Research Conference* (Society for Information Display, Playa del Rey, 1993), pp. 537–539.
14. M. S. Brennesholtz, "Light collection efficiency for light valve projection systems," in *Projection Display II*, M. H. Wu, ed., Proc. SPIE **2650**, 71–79 (1996).
15. W. J. Smith, *Modern Optical Engineering* (McGraw-Hill, New York, 1990).
16. W. T. Welford and R. Winston, *High Collection Nonimaging Optics* (Academic, San Diego, 1989).
17. Breault Research Organization, Inc., ASAP 6.0, Breault Research Organization, Inc., 6400 East Grant Road, Tucson, Ariz. 85715, USA.
18. D. M. Rutan, C. N. Stewart, and D. J. Savage, "Low wattage long lift short arc metal halide lighting systems for LCD projectors," in *Proceedings of the Sixteenth International Display Research Conference* (Society for Information Display, Santa Ana, Calif., 1996), pp. 261–264.
19. A. Csaszar, "Data projection equipment and large-screen data displays, test, and performance measurements," in *SID '91 International Symposium Digest of Technical Papers* (Society for Information Display, Playa del Rey, Calif., 1991), pp. 265–267.